1

1   The effect of elevated carbon dioxide on the sinking and swimming of the shelled pteropod

2   *Limacina retroversa*

3

4   Alexander J. Bergan[1], Gareth L. Lawson[1*], Amy E. Maas[1,2], Zhaohui Aleck Wang[3]

5

6   1. Biology Department, Woods Hole Oceanographic Institution, Woods Hole, MA,

7   USA

8   2. Bermuda Institute of Ocean Sciences, St. George's GE01, Bermuda

9   3. Marine Chemistry and Geochemistry Department, Woods Hole Oceanographic

10   Institution, Woods Hole, MA, USA

11

12 *Corresponding author: tel: +508 289 3713; e-mail:* glawson@whoi.edu

13

15

16 **Abstract**

17   Shelled pteropods are planktonic molluscs that may be affected by ocean

18   acidification. *Limacina retroversa* from the Gulf of Maine were used to investigate the

19   impact of elevated carbon dioxide (CO_2) on shell condition as well as swimming and

20   sinking behaviours. *Limacina retroversa* were maintained at either ambient (ca. 400 µatm)

21   or two levels of elevated CO_2 (800 and 1200 µatm) for up to four weeks, and then

22   examined for changes in shell transparency, sinking speed, and swimming behaviour

23   assessed through a variety of metrics (e.g., speed, path tortuosity, wing beat frequency).

24   After exposures to elevated CO_2 for as little as four days, the pteropod shells were

25   significantly darker and more opaque in the elevated CO_2 treatments. Sinking speeds were

26   significantly slower for pteropods exposed to medium and high CO_2 in comparison to the

27   ambient treatment. Swimming behaviour showed less clear patterns of response to

28   treatment and duration of exposure, but overall, swimming did not appear to be hindered

29   under elevated CO_2. Sinking is used by *L. retroversa* for predator evasion, and altered

30   speeds and increased visibility could increase the susceptibility of pteropods to predation.

31

32 **Introduction**

33   The chemistry of the oceans is rapidly changing due to the infiltration of

34   anthropogenic carbon dioxide (CO_2) into the surface ocean, a process known as ocean

35   acidification. One of the effects of ocean acidification is a decrease in the availability of

36   carbonate ion (CO_3^{2-}) which affects calcifying organisms that use calcium carbonate

37   ($CaCO_3$) to build shells and other structures (e.g. Orr *et al.* 2005, Royal Society 2005). A

38   shifting balance of dissolution and calcification as saturation state decreases due to ocean

39 acidification jeopardises the shell structure that, in many cases, provides protection from

40 predators (e.g. Fabry *et al.* 2008). Ocean acidification could also change the way that some

41 organisms move in their environment since calcified structures govern the movements of

42 certain planktonic organisms, including echinoderms and molluscs (e.g. Chan *et al.* 2011,

43 Wheeler *et al.* 2013).

44   Thecosomes, or shelled pteropods (Order Euthecosomata; henceforth referred to

45 simply as pteropods), are planktonic molluscs that build calcium carbonate shells in the

46 crystal form of aragonite, which is less stable than the other common form, calcite.

47 Pteropod shells are becoming increasingly soluble in some regions of their habitat due to

48 ocean acidification (e.g. Fabry *et al.* 2008). The shells of many species of pteropod are

49 transparent, but turn darker and more opaque when exposed to seawater under-saturated

50 with respect to aragonite, possibly due to an increased roughness of the shell's surface

51 associated with partial dissolution (Almogi-Labin *et al.* 1986, Haddad and Droxler 1996,

52 Lischka *et al.* 2011, Lischka and Riebesell 2012, Wall-Palmer *et al.* 2013). Laboratory

53 experiments have also shown that lowering the saturation state decreased calcification,

54 leading to impaired shell growth (Comeau *et al.* 2009, Comeau *et al.* 2010, Bednaršek *et*

55 *al.* 2014). Wild caught *Limacina helicina* from regions naturally low in aragonite

56 saturation state have also shown signs of dissolution under scanning electron microscopy

57 (Bednaršek, *et al.* 2012, Bednaršek, *et al.* 2014, Bednaršek, and Ohman. 2015).

58   Shelled pteropods are a food source for many marine organisms, including

59 seabirds, whales, salmon, trout, mackerel, cod, myctophids, and other zooplankton

60 (LeBrasseur 1966, Ackman *et al.* 1972, Conover and Lalli 1974, Levasseur *et al.* 1996,

61 Pakhomov *et al.* 1996, Armstrong *et al.* 2005, Hunt *et al.* 2008, Karnovsky *et al.* 2008,

62   Pomerleau *et al.* 2012, Sturdevant *et al.* 2013), and hence any effects of ocean acidification

63   on pteropod populations also could have effects on a wide range of marine species. The

64   ability of pteropods to move through the water column could be affected by ocean

65   acidification via changes to the shell. Pteropods have evolved wings, or parapodia, to

66   propel themselves through the water. The spiral shaped pteropod species (Limacinidae)

67   swim in a zig-zag motion, rotating their shell between a power stroke followed by a

68   recovery stroke to provide lift (Chang and Yen 2012, Murphy *et al.* 2016). Many species

69   of pteropods make daily migrations to depth during the day to avoid visual predators and to

70   the surface at night to feed (Wormuth 1981, Comeau *et al.* 2012, Maas *et al.* 2012);

71   sinking of the negatively buoyant shell is presumed to be an important component of the

72   downward part of this diel vertical migration. Pteropods can also use swimming and

73   sinking to escape from predators that are in their immediate proximity (Comeau *et al.*

74   2012). Harbison and Gilmer (1986) observed both swimming and sinking behaviours when

75   pteropods were disturbed. Furthermore, after pteropods die, their sinking shells sequester

76   inorganic carbon to the deep ocean (Byrne *et al.* 1984) and pteropod shells are estimated to

77   account for 12% of the global carbonate flux (Berner and Honjo 1981). Changes in the

78   fitness, abundance, and sinking of pteropods under ocean acidification thus also have

79   consequences to the carbon cycle.

80   The species examined in this study, *Limacina retroversa*, is found in the Gulf of

81   Maine, a region that is particularly susceptible to ocean acidification (Wang et al. 2013).

82   Due to deep water formation in the North Atlantic, the infiltration of anthropogenic CO_2

83   into intermediate and deep water is pronounced in this region and is causing the carbonate

84   chemistry throughout the water column to change more quickly than the average global

85   rate (Sabine *et al.* 2004). Furthermore, recent studies along the length of the U.S. East

86   Coast found that the Gulf of Maine had the lowest saturation states observed as well as the

87   lowest total alkalinity to dissolved inorganic carbon ratio, indicative of strong sensitivity to

88   continued acidification (Wang *et al.* 2013; Wanninkhof *et al.* 2015). Although found year

89   round in the Gulf of Maine, *L. retroversa* is also found in the open ocean, in the temperate

90   and subpolar Atlantic of the Northern and Southern hemispheres. As a broadly distributed

91   species that is also readily available relatively close to shore, it serves as a useful model

92   species for examining the response of pteropods to ocean acidification.

93   In this study, *L. retroversa* were captured and reared under different concentrations

94   of CO_2 over the course of multiple seasons to examine the impacts on shell condition and

95   locomotion, testing the hypotheses that 1) The appearance of shells changes after exposure

96   to elevated levels of CO_2; 2) *L. retroversa* sinking speed differs among CO_2 treatments;

97   and 3) The swimming ability of *L. retroversa* is affected by exposure to elevated CO_2.

98

99   **Methods**

100   Four cruises into the Gulf of Maine allowed for the capture of shelled pteropods,

101   *Limacina retroversa*. The pteropods were brought back to the laboratory and reared in

102   seawater modified by bubbling with three different levels of CO_2, an ambient treatment

103   (nominally 400 ppm) and two elevated treatments, 800 and 1200 ppm, hereafter referred to

104   as the ambient, medium, and high CO_2 treatments, respectively. These were intended to

105   yield over-saturated, marginal, and strongly under-saturated conditions with respect to

106   aragonite. The actual pCO_2 levels and saturation states achieved via bubbling were

107   calculated from measured dissolved inorganic carbon (DIC) and total alkalinity (TA) using

108   CO2SYS (see below). The condition of shells along with swimming performance and

109   sinking rates of animals was examined after 2 days to 4 weeks of exposure.

110

111   *Animal Sampling*

112   *Limacina retroversa* were collected in water depths of ca. 45-260 m in the Gulf of

113   Maine near Provincetown, MA aboard the R/V *Tioga* during four cruises in April, August,

114   and November 2014 and April 2015, with each expedition lasting one to three days.

115   Oblique tows were conducted with a 1-m diameter Reeve net with 333 µm mesh size. The

116   net was equipped with a large cod-end and hauled at slow speeds (ca. 5 m/min) to collect

117   animals in healthy condition. *Limacina retroversa* were isolated from the rest of the

118   plankton sample and placed into 1-L jars filled with Gulf of Maine seawater pumped *in*

119   *situ* from a depth of ca. 30 m and filtered through a 64 µm sieve. The pteropods were kept

120   at densities of ca. 30-40 individuals per litre and maintained in a refrigerator at ca. 8°C and

121   later in coolers for transfer to the laboratory.

122

123   *Culturing and Experimental Set-up*

124   Upon returning to the laboratory, *L. retroversa* were moved with a soft pipette into

125   13-L carboys with 2-3 replicate carboys per treatment. The carboys were filled with *in situ*

126   seawater collected during the cruise that had been transferred a day earlier to the laboratory

127   and filtered to 1µm. For the duration of each experiment, as well as for ca. 8-16 hours prior

128   to the addition of animals, each carboy was bubbled continuously using one of the three

129   CO_2 concentrations, ambient (nominally ca. 400 ppm), 800, and 1200 ppm. For the

130   medium and high treatments, the target air-balanced CO_2 gases used for bubbling were

131   achieved by mixing pure CO_2 gas and CO_2-free air using mass-flow controllers. The

132   ambient treatment was not controlled but rather was derived from the CO_2 content of

133   ambient air drawn from outside the building.

134   The carboys were kept in a cold room at 8°C at a density of ca. 15 individuals per

135   litre. The pteropods were fed a mixed diet of *Rhodomonas lens* (1500-4000 cells/mL) and

136   *Heterocapsa triquentra* (150-500 cells/mL) with lower concentrations provided over the

137   course of each experiment as the pteropod culture density decreased due to mortality and

138   use for various measurements. Water and pteropods were siphoned out of the carboys

139   every week so that the seawater could be replaced with clean pre-bubbled water (collected

140   *in situ* in the Gulf of Maine and kept after the cruise in a holding tank filtered continuously

141   at 1 µm) and dead pteropods could be separated from the live ones. Additional details on

142   culturing protocols can be found in Thabet *et al.* (2015).

143   During water changes, samples of the water leaving each carboy and the water

144   entering the carboys were collected in 250 mL borosilicate glass bottles, poisoned with 100

145   µL saturated mercuric chloride, and then capped with a greased stopper for later analysis of

146   TA and DIC. TA was measured using an Apollo SciTech alkalinity auto-titrator (AS-

147   ALK2, Apollo SciTech, Newark, DE, USA), an Orion 3 Star pH metre, and a Ross

148   combination pH electrode based on a modified Gran titration method (Wang and Cai

149   2004). DIC was analysed with a DIC auto-analyzer (AS-C3, Apollo SciTech, Newark, DE,

150   USA) via acidification and non-dispersive infrared CO_2 detection (LiCOR 7000: Wang and

151   Cai 2004). The saturation state of aragonite (Ω_A), pCO_2, and pH were calculated from DIC

152   and TA with the CO2SYS software (Pierrot *et al.* 2006), using constants K_1 and K_2 from

153 Mehrbach *et al.* (1973) refitted by Dickson and Millero (1987), and the KHSO$_4$

154 dissociation constant from Dickson (1990).

155   In order to monitor conditions and adjust bubbling rates accordingly between water

156 changes, pH in each carboy was measured every 2-3 days using a USB 4000 spectrometer

157 with an LS-1 light source and a FIA-Z-SMA-PEEK 100-mm flow cell (Ocean Optics,

158 Dunedin, FL, USA), and 2 mM m-Cresol indicator dye (50 µL in 20 mL of sample). The

159 DIC/TA-based calculations of Ω_A and pCO$_2$ described above were used as the primary

160 means of assessing the carbonate chemistry of the experimental treatments, but Ω_A and

161 pCO$_2$ were also calculated using CO2SYS from measurements of pH along with the

162 nearest measurement of TA in time, as a means of assessing variability between water

163 changes.

164

165   *Shell Condition*

166   Ten live animals were removed from each of the ambient, medium, and high

167 treatments at days 2, 4, 8, and 15 during the April 2015 experiment. They were rinsed in

168 deionised water, weighed wet and dry with a Cahn C-33 microbalance with a precision of

169 1 µg, then placed in 8.25% hypochlorite bleach for 24-48 hours to remove tissue, rinsed in

170 deionised water again, and dried.

171   Using a light microscope, the empty shells were photographed at 2.5X

172 magnification for transparency, opacity, and length measurements. For transparency, the

173 shell was positioned in a glass petri dish with the aperture facing up and the light coming

174 from below and through the shell. A photograph was taken through the microscope with a

175 2-ms exposure, and with white balance, contrast, and brightness values conserved across

176 images. Similarly, opacity was measured from images of shells placed with the aperture up

177 with 2-ms exposure, but with the lighting coming from two iridescent lights that

178 illuminated the shell parallel to the camera in order to measure reflected light. The lights

179 were positioned opposite each other to reduce shadows, and about 10 cm away from the

180 shell's location at the centre of the petri dish.

181 Images were analysed in MATLAB to calculate transmittance and opacity. For

182 transmittance, the shell was identified against the white background by thresholding the

183 image to black and white. The aperture as well as any holes were manually cropped from

184 the object. The transmittance was calculated as the mean grayscale value (range: 0-255) of

185 the pixels of the shell divided by 255 to get a scale of 0 (black) to 1 (white). The image

186 analysis was similar for opacity, but instead the shell was identified by thresholding the

187 brighter shell from a dark background. For opacity the mean grayscale value of the shell,

188 after cropping out the aperture and any holes, was calculated on the same scale of 0 (black)

189 to 1 (white), like transmittance.

190

191 *Videography*

192 Live and active *L. retroversa* (shell lengths ranging from 0.56 mm to 2.37 mm)

193 were removed from each of the CO_2 treated carboys for filming during the 1st, 2nd, 3rd, and

194 4th weeks of exposure to the different CO_2 treatments. Due to the length of time needed to

195 make a sufficient number of observations, filming was done over two to five days for each

196 week. The exact numbers removed from the treatments for each week as well as which

197 weeks were sampled varied among experiments due to variability in the number of live

198 animals available and needs for companion studies of physiology and gene expression. The

199   removed animals were moved to another cold room at 8°C, in 1-L jars of filtered seawater

200   at the ambient CO_2 concentration. Videos were recorded with a Photron Fastcam SA3 high

201   speed camera at 500 frames per second. A triangular prism tank with a mirrored face on

202   the hypotenuse of the isosceles right triangle was used so that both the animal and its

203   orthogonal projection were visible in the field of view and the 3D position and velocity of

204   the pteropod could be recorded (Figure 1a). Illumination was delivered by an LED panel

205   with the light diffusing through a thin plastic sheet. The mirrored tank was filled with

206   filtered seawater with a density between 1024-1026 kg/m^3. Density was measured with a

207   digital seawater refractometer (Hanna Instruments, model 96822). Three types of

208   movements were examined: sinking with wings withdrawn, sinking with wings extended,

209   and upward swimming.

210

211   *Sinking*

212   For quantification of sinking rates, a rigid pipette was attached to a ring stand and

213   placed so that the narrow end was in the water and at the top of the camera's frame (Figure

214   1b,c). The camera was focused and a ruler used to calibrate distance in the tank. The field

215   of view for sinking trials was 5.7 cm x 5.7 cm. Each *L. retroversa* was sucked into a soft

216   pipette and then released into the fixed pipette. The constriction in the fixed pipette caused

217   the animal to slow and then accelerate as it left the fixed pipette and sank through the

218   frame. Individual animals were filmed for 3-6 repeat sinking trials, which were used to

219   calculate average sinking rates for each experimental animal later used in statistical

220   comparisons among treatments. In April, August, and November of 2014, animals were

221   filmed sinking with their wings extended and also with their wings withdrawn. In April

222 2015, only animals sinking with wings withdrawn were recorded in order to dedicate more

223 time and generate a larger sample sizes for this behaviour, since by then the difference

224 between wings withdrawn and wings extended during sinking had already been

225 determined.

226   The videos were analysed in MATLAB by converting the frames to black and

227 white. With the pteropod and its reflection isolated as objects, the length and position of

228 the animal and its reflection were measured. Over successive frames, the difference in

229 position was used to calculate speed. Since the animals rotated slightly about the horizontal

230 axis the maximum length of the animal or reflection observed over the course of the video

231 was used to estimate the length of the long axis. Speed vs. time plots were fit with a

232 hyperbolic tangent function, giving an analytical solution for terminal speed. The

233 hyperbolic tangent function solves for sinking velocity for a high Reynolds number regime

234 (Owen and Ryu 2005). The Reynolds number is a non-dimensional number describing the

235 ratio of inertial to viscous forces and is calculated here as animal length multiplied by the

236 speed of the pteropod divided by the kinematic viscosity of water. Although *L. retroversa*

237 move at low to intermediate Reynolds numbers (ca. 5-50), the hyperbolic tangent function

238 fit the data better than the low Reynolds number solution (negative exponential function).

239

240   *Swimming*

241   Swimming trials were conducted by placing animals below the camera's field of

242 view via soft pipette and filming their swimming up through the frame. The size of the

243 field of view was calibrated with a ruler and was 2.7 cm x 2.7 cm, with the bottom of the

244 field of view 2-3 cm above the floor of the tank. In the April 2014 and August 2014

245   experiments, multiple pteropods from the same treatment were placed in the tank together

246   and swimming trials were recorded. Each of these swimming trials was included separately

247   in statistical comparisons among treatments, but since the exact identity of swimmers was

248   not known, the more active individuals could have contributed multiple swimming

249   observations. Therefore, for improved accuracy, in November 2014 and April 2015, a

250   single individual was placed in the tank and multiple swimming trials were recorded for

251   each animal; swimming metrics averaged over the multiple trials for each individual were

252   then used in statistical comparisons among treatments.

253   Video analysis was done in MATLAB with similar protocols as for sinking. The

254   frames were converted to black and white to allow for the identification of the pteropod

255   and its reflection to track its properties (length, position) from one frame to the next. These

256   properties were used to determine the speed, distance travelled, and trajectory. Path

257   tortuosity was measured as the total cumulative distance travelled over a video segment

258   divided by the direct distance between the last and first frame; each video segment was at

259   least 0.5 seconds and recorded at least three wing beats (power and recovery strokes). The

260   swimming metrics examined were the mean speed (calculated in 3D), frequency of wing

261   beats, path tortuosity, ratio of horizontal to vertical displacement, and asymmetry of speed

262   between the power and recovery strokes (Figure 2).

263

264   *Statistics*

265   One-way analyses of variance (ANOVA), or a Kruskal-Wallis one-way ANOVA

266   on ranks when the data failed either the equal variance or normality tests, were used to test

267   for differences among treatments in shell transmittance and opacity, sinking speeds

268   (separately for wings withdrawn and extended), swimming speed, wing beat frequency,

269   swimming path tortuosity, ratio of horizontal to vertical displacement, and asymmetry in

270   speed between the power stroke and recovery stroke. If there were significant effects from

271   these tests, post-hoc pairwise comparison tests were conducted using the Holm-Sidak

272   method for one-way ANOVAs and Dunn's method for Kruskal-Wallis one-way ANOVAs.

273   Sinking speed with wings withdrawn was compared to sinking speed with wings extended

274   using a Wilcoxon Paired-Sample Signed-Rank signed rank test. Correlation coefficients

275   were also calculated among swimming metrics.

276

277   **Results**

278   *Experimental Treatments*

279   The nominal target values for pCO_2 of 400, 800, and 1200 µatm were not always

280   achieved and calculated values varied among experiments, but overall the carbonate

281   chemistry measurements indicated clear distinctions among treatments (summarised in

282   Table 1 and see Supplementary Table S1 for full details). The ambient treatment had

283   higher levels than the nominal 400 µatm (the approximate global average atmospheric

284   concentration), closer to 450 µatm. Calculations of achieved pCO_2 for the medium and

285   high treatments also indicated variability, likely due to a combination of uncertainty in the

286   sampling and measurements of DIC and TA, uncertainty in the mixture of gas by the mass-

287   flow controllers, and variability in the degree of bubbling. In April and August 2014 the

288   calculated pCO_2 of pre-bubbled water that was entering the carboys at the onset of the

289   experiment was consistently lower than that calculated for the outgoing water, suggesting

290   incomplete pre-equilibration (Supplementary Table S1). Subsequent measurements of pH

291   made between water changes, however, indicated that the seawater chemistry for these

292   treatments attained their target values after less than 24 h.

293   Measurements of outgoing water made during water changes indicated that the

294   ambient treatments always had over-saturated conditions with respect to aragonite

295   (Ω_A=1.49-1.61), medium treatments were near the threshold of saturation (0.76 in

296   November 2014, 1.21 in August 2014, and otherwise 0.94-1.05), and the high treatment

297   had strongly under-saturated conditions (Ω_A=0.63-0.80, Table 1). The medium treatment

298   showed the greatest variability, likely due to a combination of sampling error, issues with

299   the mass-flow controllers (in November 2014, where saturation states were overly low),

300   and insufficient bubbling (in August 2014, where saturation states were overly high). The

301   ambient treatment was significantly different in aragonite saturation state from both of the

302   elevated CO_2 treatments in three of the experiments (one-way ANOVA, $p<0.001$), while in

303   the August 2014 experiment only the ambient and high treatments were significantly

304   different (Kruskal-Wallis one-way ANOVA, H=11.7, p=0.003). The medium and high

305   treatments were also significantly different from one another in April of 2014 and 2015

306   (Holm-Sidak, $p<0.05$), though not in August or November 2014. TA showed relatively

307   small differences between experiments, presumably related to natural seasonal processes in

308   the Gulf of Maine region (Supplemental Table S1).

309

310   *Shell Condition*

311   Shell condition from the April 2015 experiment for the ambient treatment was

312   mostly unchanged relative to duration of exposure, while the medium and high CO_2

313   treatments showed decreased transmittance and increased opacity over the course of 15

314 days of exposure (Figure 3, Table 2). On day 2, there was not a significant difference in the

315 appearance of shells among treatments, but both shell transmittance and opacity were

316 significantly different among treatments on days 4, 8, and 15 (Table 3). Post-hoc pairwise

317 comparisons showed that the transmittance from the ambient and high treatments were

318 significantly different on days 4, 8, and 15 ($p<0.05$), the medium and high treatments were

319 never significantly different, and the medium and ambient treatments were only

320 significantly different on day 15 ($p<0.05$). For opacity, on days 4 and 8 only the ambient

321 and high treatments were significantly different ($p<0.05$), whereas on day 15, each

322 treatment was significantly different from the others ($p<0.05$).

323   The dry masses of the shells (with animal body tissue present) from April 2015,

324 normalized to length, indicated an overall decrease over the course of the 15 days of

325 exposure and also substantial overlap among treatments (Supplementary Figure S1). Mass

326 normalized to length was significantly different between the CO_2 treatments at days 8

327 (Kruskal Wallis one-way ANOVA, H=6.1, p=0.048) and 15 (one-way ANOVA, F=4.1,

328 p=0.037), but not for the earlier time points. At day 8, there were not significant pairwise

329 differences in mass normalized to length among treatments (Dunn's method, $p>0.05$), and

330 on day 15 only the medium and high treatment were significantly different from one other

331 (Holm-Sidak method, $p<0.05$).

332

333   *Sinking*

334   Sinking rates showed differences associated with treatment, duration of exposure,

335 experiment, and behaviour (i.e. wings extended or withdrawn). After one week of

336 exposure, sinking rates for animals with wings withdrawn were similar among treatments

337 and showed no significant differences for two of three experiments (Figure 4a, Table 3),

338 while during week one of the third experiment (April 2015) sinking rates differed

339 significantly among treatments. Sinking rates were significantly slower for animals in the

340 elevated CO_2 treatments than in the ambient treatment after two or more weeks of exposure

341 during every experiment. In all pairwise comparisons, the ambient treatment was

342 significantly different from both the medium and high treatments, except for the second

343 week of the November 2014 when only the ambient and high treatments were significantly

344 different ($p<0.05$).

345   On average there was an 84% reduction in sinking speed for animals holding their

346 wings extended compared to wings withdrawn, and sinking speeds with wings withdrawn

347 and wings extended measured for the same individuals were significantly different

348 (Wilcoxon Paired-Sample Signed Rank, $Z=-8.981$, $p<0.001$). Sinking rates for animals

349 with wings extended also showed similar trends to those with wings withdrawn with

350 respect to treatment and duration of exposure (Figure 4b). While there were no significant

351 differences among the treatments after one week of exposure, significant differences were

352 observed among treatments after an exposure duration of two weeks and onwards, with

353 significantly faster sinking rates evident for the *L. retroversa* exposed to ambient CO_2

354 compared with the high treatment (November 2014 week 2) or to the medium and high

355 treatments (April 2014 week 4).

356   In order to account for possible uncertainty introduced by any differences in the

357 size of animals among treatments and time points, attempts were also made to normalise

358 the sinking rate measurements relative to individual size. Linear regressions based on log-

359 log plots were used to examine the effect of length on sinking speed of animals with wings

360   withdrawn. The resulting power law scaling relationships between sinking speed and

361   length for the ambient, medium, and high treatments were 0.45, 0.74, and 0.52 respectively

362   (Figure 5), suggesting that normalising the sinking speeds by the square root of length

363   (0.50 scaling) was appropriate. In all but one case, normalising sinking speed by length in

364   this way did not affect the significance of the differences among treatments, with the

365   exception of week one for November 2014. In this case, in contrast to the initial test, when

366   normalised, the Kruskal-Wallis one-way ANOVA showed significant differences among

367   treatments in sinking speeds (H=7.3, p=0.026) due to faster sinking in the high treatment,

368   followed by the medium, then ambient.

369

370   *Swimming*

371   In contrast to sinking, swimming rates did not differ in a consistent manner among

372   treatments and durations of exposure. For the two experiments (August 2014 and April

373   2015) where observations were made after one week, mean swimming speed was

374   significantly different among treatments but differed in which treatment showed the fastest

375   swimming (Figure 6a, Table 3). Significant differences were not seen among treatments at

376   two or three weeks. There was also not a significant correlation between swimming speed

377   and animal length (Table 4): in the log-log plot of swimming speed vs. animal length the

378   slopes of the linear regressions were nearly zero (see Supplementary Figure S2) and hence

379   no attempts were made to normalise swimming measurements to animal size.

380   For the initial two experiments (April and August 2014) where multiple animals

381   were together in the filming tank and individual swim analyses were not possible, wing

382   beat frequency showed no differences among treatments (Figure 6b, Table 3). For the two

383 later experiments (November 2014 and April 2015), where individual animals were

384 measured separately, a trend of decreasing flapping frequency under elevated CO_2 was

385 evident, and the frequency of wing beats was significantly higher in the ambient treatment

386 compared to the medium and high treatments in week one of the April 2015 experiment,

387 although not in week two of the November 2014 experiment or week two of April 2015.

388   Tortuosity only differed significantly during the initial experiments (April 2014 and

389 August 2014), where multiple animals were placed together during filming (Figure 6c,

390 Table 3). In the November 2014 and April 2015 experiments, no significant differences

391 were seen in tortuosity among the treatments, although there was a high degree of

392 variability during the November 2014 week two experiment, where the ambient treatment

393 had the highest tortuosity due to an outlier (4.05) and low sample size (n=3). The average

394 ratio of horizontal to vertical displacement averaged over all the experiments was

395 0.35±0.15 (±standard deviation) and similar to tortuosity there were only significant

396 differences between treatments in April 2014 (Kruskal-Wallis one-way ANOVA, H=8.7,

397 p=0.013) and August 2014 (Kruskal-Wallis one-way ANOVA, H=6.9, p=0.032). The

398 asymmetry between the peak speeds of the power and recovery strokes did not differ

399 among treatments for any of the experiments (one-way ANOVA). The average and

400 standard deviation of asymmetry between the power/recovery strokes over all the

401 experiments was 7.2±5.1% (n=191).

402   There was a significant positive correlation between mean swimming speed and

403 wing beat frequency and a significant negative correlation between wing beat frequency

404 and length (Table 4). The mean swimming speed also had significant negative correlations

405 with both tortuosity and the asymmetry between the speeds of the power and recovery

406 strokes. There were no significant correlations between tortuosity or the asymmetry of the

407 strokes and length.

408

409 **Discussion**

410 The condition of *Limacina retroversa* shells and sinking speeds of live animals

411 were significantly affected by exposure to elevated carbon dioxide. Since the passive

412 motion of sinking was slower in the elevated CO_2 treatments, even for animals with wings

413 withdrawn, this indicates that the slower sinking rates likely relate to differences in the

414 shells. Swimming behaviour showed less clear patterns of variability in relation to

415 treatment and duration of exposure, and overall swimming ability did not appear to be

416 hindered under elevated CO_2.

417

418 *Shell Condition*

419 The appearance of shells changed significantly in the elevated CO_2 treatments.

420 Differences in transmittance and opacity of the shells from the medium and high

421 treatments relative to the ambient treatment were apparent from day four of exposure,

422 while in contrast the shells from the ambient treatment did not change significantly over

423 time. Other studies have found that short exposures to similar CO_2 concentrations (750,

424 880, and 1000 ppm for 7-8 days) can cause changes in shell condition of *L. retroversa*

425 (Lischka and Riebesell 2012, Manno *et al.* 2012) and in the congeneric species *L. helicina*

426 (Lischka *et al.* 2011, Bednaršek *et al.* 2012, Busch *et al.* 2014, Bednaršek *et al.* 2014). The

427 present study adds to these earlier observations by offering a new, quantitative metric for

428 assessing shell condition based on transparency to light-based microscopy and by

429   extending the duration over which effects on shell condition were examined. Although

430   they were measured and considered separately, transmittance and opacity are highly related

431   optical properties and as such expectedly showed very similar patterns (though in opposing

432   directions). Future studies employing our light microscopy-based approach might thus

433   focus on transmittance, since the transverse lighting used for opacity measurements causes

434   some glare on the shells regardless of condition which may affect the sensitivity of this

435   metric.

436   A loss of transparency could have a negative impact on shelled pteropods since

437   transparency is a form of camouflage in the open ocean environment. Although some

438   pteropod predators, notably the gymnosome (or shell-less) pteropods, are non-visual, the

439   decrease in transparency could potentially serve to increase visibility to visual predators

440   known to feed on pteropods, such as fish and birds (LeBrasseur 1966, Levasseur *et al.*

441   1996, Armstrong *et al.* 2005, Hunt *et al.* 2008, Karnovsky *et al.* 2008, Sturdevant *et al.*

442   2013). It is not known how small of a change in CO_2 concentration will elicit a response in

443   shell condition, but it is noteworthy that changes were evident here in the medium

444   treatment, which in April 2015 was just above an aragonite saturation state of one, a

445   potential environmental threshold. The loss of transparency is likely caused by dissolution

446   of the calcium carbonate matrix, as has been seen at higher resolution using scanning

447   electron microscopy (e.g. Bednaršek *et al.* 2012). It is possible that the more gradual

448   change in CO_2 concentrations that will occur as a result of climate change could allow for

449   adaptation, although shell dissolution has already been documented for wild populations of

450   *L. helicina* exposed to naturally low saturation state conditions (Bednaršek *et al.* 2012,

451   Bednaršek *et al.* 2014). The methods provided here for examining the transparency of

452 shells could be applied to natural populations to look for seasonal and inter-annual

453 changes.

454

455   *Sinking*

456   Although sinking speeds have been previously quantified in some pteropod species

457 (Lalli and Gilmer 1989), the effect of elevated CO_2 on pteropod sinking has not previously

458 been examined, despite the important role that sinking plays in pteropod locomotion and

459 carbonate flux. In this study, the sinking speeds of *L. retroversa* were slower during the

460 second week of exposure to elevated CO_2 and onwards. Measurements of mass made for

461 the April 2015 experiment, normalized to length to account for variability in size, did not

462 indicate a clear pattern among treatments indicative of dissolution due to exposure to

463 enhanced CO_2. It is thus not clear whether the change in sinking speed are due to the shells

464 changing in mass, density, or if they are modified in a way that increases drag. It is also not

465 known whether the experimentally manipulated chemical conditions had any impacts on

466 the mass of the animal bodies, separate from the shells. Given the relatively massive shells

467 and direct linkage between under-saturated conditions and calcium carbonate dissolution,

468 however, it seems likely that changes in sinking speed relate primarily to changes in the

469 shells. The ambient treatment also showed slower sinking with increased duration of

470 exposure, but nonetheless the effect of elevated CO_2 treatment was persistent and sinking

471 both with wings withdrawn and extended showed a similar treatment effect. The decrease

472 in sinking speed for the ambient treatment could indicate a captivity effect, where animals

473 in all treatments might decrease in overall health and vigour with increased duration of

474 time in captivity. It could also be due to removal of larger individuals earlier in the

22

475   experiments, leading to smaller pteropods being tested in the later weeks, although the

476   effect of exposure on sinking speed was consistent when normalised by the square root of

477   length (based on the observed relationship between size and sinking speed) so this is less

478   likely. In an earlier study, the scaling between shell length and sinking speed for the

479   congeneric species *L. helicina* was between 0.3 and 0.4 (Chang and Yen, 2012), similar to

480   the scaling of 0.5 found in this study. Animal length and speed are also important in

481   determining the Reynolds number (Re). Since *L. retroversa* moves in a transitional regime

482   of Re between ca. 5 and 50, decreases in sinking and swimming speeds might lead to a

483   decrease in Re that could result in increased viscous drag (Walker 2002).

484   Extended wings slowed sinking, presumably as an adaptation to minimise energetic

485   expenditure on swimming to maintain position in the water column. In the laboratory, our

486   observation is that pteropods alternate periods of swimming upwards with sinking, while in

487   the field, the production of mucous webs is thought to slow or even halt sinking, although

488   the prevalence of this behaviour is not well known (Gilmer and Harbison 1986). The bio-

489   energetic consequences to pteropods in the wild of reduced sinking speeds are thus

490   somewhat difficult to assess, but it may be that metabolic costs of maintaining position in

491   the water column are overall reduced under exposure to enhanced CO_2. In contrast,

492   changes in sinking speed may have negative consequences in terms of vulnerability to

493   predation. The gymnosome pteropods feed exclusively on shelled pteropods and for this

494   monospecific predator-prey relationship, withdrawing wings into the shell might make it

495   harder for the predatory shell-less pteropods to successfully capture and consume their

496   prey (Conover and Lalli 1974). Sinking behaviour in the wild is also believed to be a mode

497   of predator avoidance: a response to a disturbance was noted for the pteropod species

498 *Diacria quadridentata*, which withdrew its wings presumably to achieve a faster sinking

499 speed (Gilmer and Harbison 1986). Overall, there are only a few field observations of

500 pteropod behaviour in the wild, but along with the decrease in transparency and

501 camouflage, a decrease in sinking speed with increased CO_2 is another way that *L.*

502 *retroversa* and other shelled pteropods might have increased vulnerability to predators due

503 to ocean acidification.

504 Post-mortem sinking of pteropod shells is important for the biogeochemical cycling

505 of carbon (Berner and Honjo 1981). The solubility of aragonite increases with depth,

506 dropping below a saturation state of one at a depth known as the aragonite compensation

507 depth, which is shoaling due to ocean acidification (Fabry *et al.* 2008). Dissolution is not

508 immediate below the aragonite compensation depth, however, and shells that sink more

509 slowly have more time to be dissolved before reaching deeper water (Byrne *et al.* 1984).

510 The combination of the slower sinking rates observed here with the shoaling of the

511 compensation depth and the elevated rate of dissolution expected from ocean acidification

512 is likely to cause pteropod dissolution and redistribution of carbonate to occur at

513 increasingly shallower depths.

514

515 *Swimming*

516 Although the degradation of the shell after exposure to elevated CO_2 might have

517 been expected to have consequences to the animal's weight and ballast, swimming

518 behaviour did not show clear changes when *L. retroversa* were exposed to elevated CO_2.

519 In particular, unlike sinking speed, swimming speed did not show any clear reduction in

520 the elevated CO_2 treatments. It may be that the differences among the experiments in

521 swimming behaviour and the sensitivity of the various swimming metrics to CO_2 relate to

522 seasonal differences in the overall condition, developmental state, and vigour of the

523 animals prior to capture that persisted through the experiments; these differences may also

524 be influenced by overall low sample sizes. It should also be noted that variability in

525 individual swimming performance may have affected the patterns evident in the April and

526 August 2014 experiments, where multiple animals were present in the filming tank

527 concurrently, relative to the multiple runs done on individual animals in the November

528 2014 and April 2015 experiments. This methodological change was unfortunate and

529 introduces the possibility of pseudo-replication in the earlier two experiments if swimming

530 was observed for the same animal more than once. Given the overall low sample sizes and

531 dearth of previous information, we have presented the observations from both the initial

532 sub-optimal experiments as well as the latter two more rigorous investigations. No

533 consistent differences across the measured swimming metrics were evident associated with

534 the change in method.

535   The significant differences in swimming speed in the first week of exposure may be

536 spurious, as the treatment with the fastest swimmers was not consistent among experiments

537 and significant differences among treatments did not persist after longer exposure

538 durations. A previous study by Manno *et al.* (2012) manipulated CO_2 and salinity to

539 examine how swimming was affected in *L. retroversa* and found that elevated CO_2 alone

540 did not cause a change in swimming speed or wing beat frequency after eight days of

541 exposure, while decreased salinity combined with increased CO_2 conditions slowed the

542 swimming and increased the beat frequency. This supports the idea that our findings at one

543 week are spurious.

544   More consistent in the present study than the patterns in swimming speed was a

545   trend towards decreased wing beat frequency in the medium and high treatments relative to

546   ambient, albeit only significant in one of the experiments. This reduction in wing beat

547   frequency is interesting in its not being accompanied by an associated difference between

548   treatments in swimming speed (although at the individual level, wing beat frequency was

549   positively correlated with swimming speed). A reduction in beat frequency may suggest a

550   reduced metabolic cost of swimming in the animals exposed to elevated CO_2, and is

551   perhaps associated with a less massive shell. While there was not a good correlation

552   between swimming speed and length, there was a significant negative correlation between

553   wing beat frequency and length, which has also been noted in another study where larger

554   *L. helicina* beat their wings less frequently but achieved greater speeds (Chang and Yen

555   2012). That more detailed study of swimming kinetics also found that across sizes the

556   trajectory and timing of the wing strokes varied, possibly as a response to changing

557   Reynolds number regimes.

558   Tortuosity often, but not always, showed differences associated with treatment in

559   the present study, with greatest tortuosity in the ambient treatment. Tortuosity was

560   significantly negatively correlated to swimming speed, as animals tended to exhibit more

561   horizontal movements that often appeared helical in nature when swimming at lower

562   speeds. Tortuosity and length were also negatively related, though not quite significantly.

563   Chang and Yen (2012) similarly found that the helical component of *L. helicina* swimming

564   paths was greater for larger individuals. Pteropod swimming relies on the rotation of the

565   shell between the power and recovery strokes and differential dissolution along the

566   elongate shells of individual *L. retroversa* could conceivably influence swimming

567   efficiency. Examining the asymmetry in swimming speed induced by the power and

568   recovery strokes, however, did not show any effect of CO_2 exposure. In general it is

569   possible that the limited effects observed on the swimming metrics examined here in

570   relation to CO_2 exposure are due to shell dissolution (and associated potential impacts on

571   weight and ballast) not being advanced enough to result in discernible consequences to

572   swimming. If future studies can overcome limitations in the durations over which

573   pteropods can be maintained in captivity, the longer-term effects on locomotion of

574   enhanced CO_2 might be examined.

575

576   **Conclusions**

577   This study observed decreased sinking speeds in pteropods exposed to conditions

578   of elevated CO_2 that could exist by the end of the century, suggesting that ocean

579   acidification could affect pteropod fitness, as sinking is a mode of predator avoidance.

580   Decreased sinking speeds will likely also slow the passive transport of calcium carbonate

581   to depth. Ocean acidification could potentially also increase the visibility of pteropods to

582   predators, since increased CO_2 significantly affected the transparency of shells. Longer

583   perturbation experiments or greater replication may be needed to understand whether

584   ocean acidification affects swimming. The cues that pteropods respond to that motivate

585   their upward swimming are not known, and whether these cues are influenced by CO_2

586   treatment is also uncertain. Overall, more behavioural experiments on pteropods are

587   needed to understand the consequences of ocean acidification, although this relies on the

588   development of improved culture techniques in order to achieve adequately large sample

589   sizes and to examine impacts over longer time periods (Howes *et al.* 2015).

590

Supplementary Materials

Supplementary material is available at ICES JMS online, including figures of shell mass

measurements normalized to length vs. exposure duration for the April 2015 experiment

and swimming speed vs. length as well as a table providing the full carbonate chemistry

measurements and calculations. MATLAB code for the analysis of pteropod shell

transmittance and opacity is available at http://www.bco-dmo.org/project/2263.

597

28

612   Ocean Institute, Pickman Foundation, and the Tom Haas Fund at the New Hampshire

613   Charitable Foundation.

614
615   **References**

616
617   Ackman, R.G., Hingley, J., and MacKay, K.T. 1972. Dimethyl sulfide as an odor component in Nova Scotia
618   fall mackerel. *Journal of Fisheries Research Board of Canada*. 29: 1085-1088.

619   Almogi-Labin, A., Luz, B., Duplessy, J.-C. 1986. Quaternary paleo-oceanography, pteropod preservation and
620   stable-isotope record of the Red Sea. *Palaeogeography, Palaeoclimatology, Palaeoecology*. 57:
621   195-211.

622   Armstrong, J.L., Boldt, J.L., Cross, A.D., Moss, J.H., Davis, N.D., Meyers, K.W., Walker, R.V., *et al*. 2005.
623   Distribution, size, and interannual, seasonal and diel food habits of northern Gulf of Alaska juvenile
624   pink salmon, *Oncorhynchus gorbuscha*. *Deep-Sea Research II: Tropical Studies in Oceanography*.
625   52: 247-265.

626   Bednaršek, N., Tarling, G.A., Bakker, D.C., Fielding, S., Jones, E.M., Venables, H.J., Ward, P., *et al*. 2012.
627   Extensive dissolution of live pteropods in the Southern Ocean. *Nature Geoscience*. 5: 881-885.

628   Bednaršek, N., Feely, R.A., Reum, J.C.P., Peterson, B., Menkel, J., Alin, S.R., and Hales, B. 2014. *Limacina*
629   *helicina* shell dissolution as an indicator of declining habitat suitability owing to ocean acidification
630   in the California Current Ecosystem. *Proceedings of the Royal Society B*. 281: 20140123.

631   Bednaršek, N., and Ohman, M.D. 2015. Changes in pteropod distributions and shell dissolution across a
632   frontal system in the California Current System. *Marine Ecology Progress Series*. 523: 93-103.

633   Berner, R.A., and Honjo, S. 1981. Pelagic sedimentation of aragonite: its geochemical significance. *Science*.
634   211(4485): 940-942.

635   Busch, D.S., Maher, M., Thibodeau, P., and McElhany, P. 2014. Shell condition and survival of Puget Sound
636   pteropods are impaired by ocean acidification conditions. *PLoS ONE*. 9(8): e105884. doi:
637   10.1371/journal.pone.0105884.

638   Byrne, R.H., Acker, J.G., Betzer, P.R., Feely, R.A., and Cates, M.H. 1984. Water column dissolution of
639   aragonite in the Pacific Ocean. *Nature*. 312: 322-326.

640   Chan, K.Y.K., Grünbaum, D., and O'Donnell, M.J. 2011. Effects of ocean acidification induced
641   morphological changes on larval swimming and feeding. *The Journal of Experimental Biology*. 214:
642   3857-3867.

643   Chang, Y., and Yen, J. 2012. Swimming in the intermediate Reynolds range: kinematics of the pteropod
644   *Limacina helicina*. *Integrative and Comparative Biology*. 52(5): 597-615.

645   Comeau, S., Gorsky, G., Jeffree, R., Teyssié, J.L., and Gattuso, J.P. 2009. Key arctic pelagic mollusk
646   (*Limacina helicina*) threatened by ocean acidification. *Biogeosciences*. 6: 1877-1882.

647   Comeau, S., Jeffree, R., Teyssié, J.L., and Gattuso, J.P. 2010. Response of the Arctic pteropod *Limacina*
648   *helicina* to projected future environmental conditions. *PLoS ONE*. 5(6): e11362. doi:
649   10.1371/journal.pone.0011362.

650   Comeau, S., Alliouane, S., and Gattuso, J.P. 2012. Effects of ocean acidification on overwintering juvenile
651   Arctic pteropods *Limacina helicina*. *Marine Ecology Progress Series*. 456: 279-284.

652   Conover, R.J., and Lalli, C.M. 1974. Feeding and growth in *Clione limacina* (Phipps), a pteropod mollusk. II.
653   Assimilation, metabolism, and growth efficiency. *Journal of Experimental Marine Biology and*
654   *Ecology*. 16: 131-154.

655   Dickson, A.G., and Millero, F.J. 1987. A comparison of the equilibrium constants for the dissociation of
656   carbonic acid in seawater media. *Deep Sea Research*. 34: 1733-1743.

29

657 Dickson, A.G. 1990. Thermodynamics of the dissociation of boric acid in synthetic seawater from 273.15 to
658   318.15 K. *Deep Sea Research.* 37: 755-766.

659 Fabry, V.J., Seibel, B.A., Feely, R.A., and Orr, J.C. 2008. Impacts of ocean acidification on marine fauna and
660   ecosystem processes. *ICES Journal of Marine Science*. 65: 414 -432.

661 Gilmer, R.W., and Harbison, G.R. 1986. Structure and field behavior of pteropod molluscs: feeding methods
662   in the families Cavoliniidae, Limacinidae, and Peraclididae (Gastropoda: Thecosomata). *Marine*
663   *Biology*. 91: 47-57.

664 Haddad, G.A., and Droxler, A.W. 1996. Metastable $CaCO_3$ dissolution at intermediate water depths of the
665   Caribbean and western North Atlantic: Implications for intermediate water circulation during the
666   past 200,000 years. *Paleoceanography.* 11(6): 701-716.

667 Hunt, B.P.V., Pakhomov, E.A., Hosie, G.W., Siegel, V., Ward, P., and Bernard, K. 2008. Pteropods in the
668   southern ocean ecosystems. *Progress in Oceanography*. 78: 193-221.

669 Karnovsky, N.J., Hobson, K.A., Iverson, S., and Hunt, G.L. 2008. Seasonal changes in diets of seabirds in
670   the North Water Polynya: a multiple-indicator approach. *Marine Ecology Progress Series.* 357: 291-
671   299.

672 Lalli, C.M., and Gilmer, R.W. 1989. Pelagic snails: the biology of holoplanktonic gastropod mollusks.
673   *Stanford University Press*, Los Altos. 259 pp.

674 LeBrasseur, R.J. 1966. Stomach contents of salmon and steelhead trout in the Northeastern Pacific Ocean.
675   *Journal of Fisheries Research Board of Canada*. 23(1): 85-100.

676 Levasseur, M., Keller, M.D., Bonneau, E., D'Amours, D., and Bellows, W.K. 1994. Oceanographic basis of
677   a DMS-related Atlantic cod (Gadus morhua) fishery problem: blackberry feed. *Canadian Journal of*
678   *Fisheries and Aquatic Sciences*. 51: 881-889.

679 Lischka, S., Büdenbender, J., Boxhammer, T., and Riebesell, U. 2011. Impact of ocean acidification and
680   elevated temperatures on early juveniles of the polar shelled pteropod *Limacina helicina*: mortality,
681   shell degradation, and shell growth. *Biogeosciences*. 8: 919-932.

682 Lischka, S., and Riebesell, U. 2012. Synergistic effects of ocean acidification and warming on overwintering
683   pteropods in the Arctic. *Global Change Biology*. 18: 3517-3528.

684 Maas, A.E., Wishner, K.F., and Seibel, B.A. 2012. Metabolic suppression in thecosomatous pteropods as an
685   effect of low temperature and hypoxia in the eastern tropical North Pacific. *Marine Biology*. 159:
686   1955-1967.

687 Manno, C., Morata, N., and Primicerio, R. 2012. *Limacina retroversa's* response to combined effects of
688   ocean acidification and sea water freshening. *Estuarine, Coastal and Shelf Science*. 113: 163-171.

689 Mehrbach, C., Culberson, C.H., Hawley, J.E., and Pytkowicz, R.M. 1973. Measurement of apparent
690   dissociation constants of carbonic acid in seawater at atmospheric pressure. *Limnology and*
691   *Oceanography*. 18: 897-907.

692 Murphy, D.W., Adhikari, D., Webster, D.R., and Yen, J. 2016. Underwater flight by the planktonic sea
693   butterfly. *Journal of Experimental Biology*. 219: 535-543.

694 Orr, J.C., Fabry, V.J., Aumont, O., Bopp, L., Doney, S.C., Feely, R.A., and Gnanadesikan, A., *et al*. 2005.
695   Anthropogenic ocean acidification over the twenty-first century and its impacts on calcifying
696   organism. *Nature.* 437(29): 681-686.

697 Owen, J.P., and Ryu, W.S. 2015. The effects of linear and quadratic drag on falling spheres: an
698   undergraduate laboratory. *European Journal of Physics*. 26: 1085-1091.

699 Pakhomov, E.A., Perissinotto, R., and McQuaid, C.D. 1996. Prey composition and daily rations of myctophid
700   fishes in the Southern Ocean. *Marine Ecology Progress Series.* 134: 1-14.

701 Pierrot, D., Lewis, E., and Wallace, D. 2006. Co2sys DOS Program developed for CO_2 system calculations.
702   Carbon Dioxide Information anlysis Center, Oak Ridge National Laboratory, US Department of
703   Energy ORNL/CDIAC-105.

704 Pomerleau, C., Lesage, V., Ferguson, S.H., Winkler, G., Petersen, S.D., and Higdon, J.W. 2012. Prey
705   assemblage isotopic variability as a tool for assessing diet and the spatial distribution of bowhead
706   whale *Balaena mysticetus* foraging in the Canadian eastern Arctic. *Marine Ecology Progress Series.*
707   469: 161-174.

708 Royal Society. 2005. Ocean acidification due to increasing atmospheric carbon dioxide. *Policy Document*
709   *12/05, The Royal Society.*

710 Sabine, C.L., Feely, R.A., Gruber, N., Key, R.M., Lee, K., Bullister, J.L., Wanninkhof, R., *et al*. 2004. The
711   oceanic sink for anthropogenic CO_2. *Science*. 305(5682): 367-371.

712 Sturdevant, M.V., Orsi, J.A., and Fergusson, E.A. 2013. Diets and trophic linkages of epipelagic fish
713   predators in coastal Southeast Alaska during a period of warm and cold climate years, 1997-2011.
714   *Marine and Coastal Fisheries: Dynamics, Management, and Ecosystem Science*. 4: 526-545.

715 Thabet, A.A., Maas, A.E., Lawson, G.L., and Tarrant, A.M. 2015. Life cycle and early development of the
716   thecosomatous pteropod *Limacina retroversa* in the Gulf of Maine, including the effect of elevated
717   CO_2 levels. *Marine Biology*. 162: 2235-2249.

718 Walker, J.A. 2002. Functional Morphology and Virtual Models: Physical Constraints on the Design of
719   Oscillating Wings, Fins, Legs, and Feed at Intermediate Reynolds Numbers. *Integrative and*
720   *Comparative Biology*. 42: 232-242.

721 Wall-Palmer, D., Smart, C.W., and Hart, M.B. 2013. In-life pteropod shell dissolution as an indicator of past
722   ocean carbonate saturation. *Quaternary Science Reviews*. 81: 29-34.

723 Wanninkhof, R., Barbero, L., Byrne, R., Cai, W.J., Huang, W.J., Zhang, J.Z., Baringer, M., and Langdon, C.
724   2015. Ocean acidification along the Gulf Coast and East Coast of the USA. *Continental Shelf*
725   *Resesarch*. 98: 54-71.

726 Wang, Z.A., and Cai W.J. 2004. Carbon dioxide degassing and inorganic carbon export from a marsh-
727   dominated estuary (the Duplin River): a marsh CO_2 pump. *Limnology and Oceanography*. 49: 341-
728   354.

729 Wang, Z.A., Wanninkhof, R., Cai, W.J., Byrne, R.H., Hu, X., Peng, T.H., and Huang, H.J. 2013. The marine
730   inorganic carbon system along the Gulf of Mexico and Atlantic coasts of the United States: insights
731   from transregional coastal carbon study. *Limnology and Oceanography*. 58(1): 325-342.

732 Wheeler, J.D., Helfrich, K.R., Anderson, E.J., McGann, B., Staats, P., Wargula, A.E., Wilt, K., and
733   Mullineaux, L.S. 2013. Upward swimming of competent oyster larvae *Crassostrea virginica* persists
734   in highly turbulent flow as detected by PIV flow subtraction. *Marine Ecology Progress Series*. 488:
735   171-185.

736 Wormuth, J.H. 1981. Vertical distributions and diel migrations of *Euthecosomata* in the northwest Sargasso
737   Sea. *Deep-sea Research*. 28A(12): 1493-1515.

738

739 **Captions**

740 Figure 1. (a) Schematic of the filming set up. The seawater tank had a mirror to show the

741 actual and reflected image of an animal sinking or swimming, allowing position to be

742 determined in three dimensions. A high speed camera was used for filming and

743 illumination was provided by an LED panel. The tank was 10 cm long, 10 cm wide, and 10

744 cm high. (b) Filming set up showing the mirrored tank with the fixed pipette that was used

745 to drop the pteropods through for sinking trials. (c) One frame of a video shows the actual

746 image and mirrored image of a sinking pteropod with wings withdrawn, shortly after

747 exiting the fixed pipette.

748

749 Figure 2. (a) Speed vs time plot of a swimming trial, showing the full time-series of speed

750 from the 3 second video segment (blue), along with calculated mean speed (red line), a

751 wing beat period, and the asymmetry in peaks. The wing beat frequency was calculated as

752 1/(beat period) and included both the power and recovery strokes. Power strokes were

753 consistently associated with greater speeds and asymmetry between the peak speeds of the

754 power and recovery stroke was measured as the difference between subsequent peaks of

755 speed divided by the larger of the two. (b) The 3D trajectory of a swimming *L. retroversa*

756 shows the pattern of motion. Note that this is a scatter plot but the high frame rate of the

757 camera leads to the points appearing essentially as a line. Tortuosity was calculated as the

758 total cumulative distance traveled divided by the direct distance from starting point to

759 finish.

760

761 Figure 3. (a) Transmittance (proportion of transmitted light) and (b) opacity (proportion of

762 reflected light) of *L. retroversa* shells from the April 2015 experiment relative to duration

763 of exposure for each of the three CO_2 treatments.

764

765 Figure 4. (a) Terminal sinking speed for *L. retroversa* with wings withdrawn for the four

766 experiments (circle: April 2014; square: August 2014; diamond: November 2014; triangle:

767 April 2015) after durations of exposure of 1-4 weeks. From left to right within each weekly

768 bracket the ambient, medium, and high treatment are plotted, although the treatments were

769 measured together of the course of 2-5 days and are spaced along the x-axis simply for

770 easier visualisation. The error bars denote standard error. (b) The terminal sinking speed

771 with wings extended for the April 2014, August 2014, and November 2015 experiments.

772 No measurements of sinking with wings extended were made in April 2015 or in week 3 of

773 any of the experiments.

774

775 Figure 5. Log_{10} terminal sinking speed with wings withdrawn vs log_{10} shell length for each

776 treatment (points) along with a linear regression for each treatment (lines). The slope of the

777 linear regressions shows the power scaling between sinking speed and shell length.

778 Contours of constant Reynolds numbers (Re) of 5, 10, and 20 are shown in black.

779

780 Figure 6. (a) Mean swimming speed, (b) wing beat frequency, and (c) tortuosity for *L.*

781 *retroversa* for the four experiments (circle: April 2014; square: August 2014; diamond:

782 November 2014; triangle: April 2015) after durations of exposure of 1-3 weeks. From left

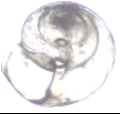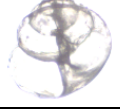783 to right within a week the ambient, medium, and high treatment are plotted, although
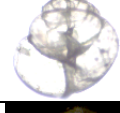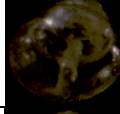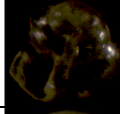
784   treatments were measured together over the course of 2-5 days. The error bars denote

785   standard error. Both the power and recovery stroke are included in each wing beat in

786   calculating wing beat frequency.

787

788 Table 1. The carbonate chemistry parameters partial pressure of CO_2 (pCO_2), pH, and aragonite saturation
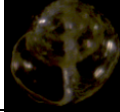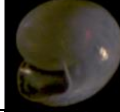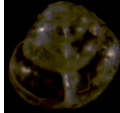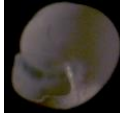789 state (Ω_A) are average values for the water leaving the treatment carboys at days 7 and 14 during water
790 changes. TA and DIC were directly measured and were used for calculation of the other parameters.
791 Measurements of ingoing water at the start of each week of exposure in April and August 2014 appeared to
792 indicate insufficient pre-equilibration, although target levels were reached by day 1 (see text and
793 Supplementary Table S1). The values are reported as the mean ± standard deviation.
794

Experiment	Treatment	pCO_2 (µatm)	pH	Ω_A
April 2014	Ambient	470±20	7.96±0.02	1.54±0.06
	Medium	850±40	7.73±0.02	0.94±0.03
	High	1190±120	7.59±0.04	0.70±0.07
Aug 2014	Ambient	440±40	7.98±0.03	1.58±0.11
	Medium	650±170	7.84±0.11	1.21±0.30
	High	990±100	7.66±0.04	0.80±0.08
Nov 2014	Ambient	480±50	7.95±0.04	1.49±0.11
	Medium	1100±290	7.63±0.10	0.76±0.15
	High	1320±160	7.55±0.05	0.63±0.07
April 2015	Ambient	440±30	7.99±0.03	1.61±0.09
	Medium	740±100	7.78±0.05	1.05±0.12
	High	1180±190	7.59±0.07	0.70±0.11

795

796 Table 2. Representative images showing the changes in
797 shell appearance from day 2 to day 15 for each treatment
798 during the April 2015 experiment. Transmittance images
799 are taken when light is shining from below the sample,
800 and opacity images are taken when light is illuminating
801 the sample from the sides.
802

	Treatment	Day 2	Day 15
Transmittance	Ambient		
	Medium		
	High		
Opacity	Ambient		
	Medium		
	High		

803
804

805 Table 3. Cruise and experiment details and associated statistics. For each type of observation of *L. retroversa* (shell condition, sinking, or swimming) and each
806 duration of exposure the sample sizes are listed (ambient, medium, high). Test statistics (F for one-way ANOVAs and H for Kruskal-Wallis one-way ANOVAs
807 on ranks) are reported for comparisons among treatments for multiple sinking, swimming, and shell variables abbreviated as follows: "Sinking wings in" is
808 sinking speed with wings withdrawn, "Sinking wings out" is sinking speed with wings extended, "Swim speed" is mean swimming speed, "Beat" is wing beat
809 frequency, and "Tort" is tortuosity. * $p<0.05$, ** $p<0.01$, *** $p<0.001$, NS=Non-Significant
810
811

Experiment	Cruise Dates	Type of Observation	Exposure Duration	Sample Size Amb., Med., High	One-way ANOVA: F Kruskal-Wallis one-way ANOVA: H
April 2014	25 April – 27 April 2014	Sinking	4 Weeks	10, 10, 7	Sinking wings in: F=9.8***; Sinking wings out: F=9.0**
		Swimming	3 Weeks	11, 7, 10	Swim speed: F=0.9^{NS}, Beat: H=1.7^{NS}, Tort: H=8.4*
August 2014	19 August 2014	Sinking	1 Week	10, 12, 13	Sinking wings in: H=1.1^{NS}, Sinking wings out: F=1.0^{NS}
		Swimming	1 Week	13, 21, 17	Swim speed: F=4.6*, Beat: H=2.1^{NS}, Tort: H=10.6**
November 2014	4 November – 6 November 2014	Sinking	1 Week	20, 22, 20	Sinking wings in: F=0.3^{NS}, Sinking wings out: F=0.4^{NS}
		Sinking	2 Weeks	25, 20, 18	Sinking wings in : F=4.2*, Sinking wings out : F=6.4**
		Swimming	2 Weeks	3, 10, 10	Speed: H=1.6^{NS}, Beat: F=1.6^{NS}, Tort: H=2.3^{NS}
April 2015	26 April – 27 April 2015	Sinking	1 Week	25, 26, 25	Sinking wings in: F=5.8**
		Sinking	2 Weeks	26, 26, 22	Sinking wings in: H=11.6**
		Sinking	3 Weeks	26, 22, 16	Sinking wings in: F=19.0***
		Swimming	1 Week	15, 18, 16	Swim speed: F=3.7*, Beat: F=9.5***, Tort: H=4.7^{NS}
		Swimming	2 Weeks	8, 14, 18	Swim speed: F=0.1^{NS}, Beat: F=1.5^{NS}, Tort: H=5.1^{NS}
		Shells	2 Days	8, 9, 8	Transmittance: F=0.1^{NS}, Opacity: H=0.8^{NS}
		Shells	4 Days	8, 8, 8	Transmittance: H=9.0*, Opacity: H=8.1*
		Shells	8 Days	8, 7, 5	Transmittance: H=14.5***, Opacity: H=13.0**
		Shells	15 Days	7, 7, 5	Transmittance: F=60***, Opacity: F=212***

812 Table 4. Correlation coefficients (r) among the swimming variables: mean swimming speed, wing beat
813 frequency, path tortuosity, and asymmetry between the peaks of speed (i.e. the difference between the power
814 and recovery stroke). Bold indicates significant correlations. * p<0.05, ** p<0.01, *** p<0.001, NS=Non-
815 Significant

Correlation coefficient	Length	Wing Beat frequency	Tortuosity	Asymmetry in peaks
Speed	0.0005[NS]	**0.2395 *****	**-0.4357*****	**-0.18233***
Length		**-0.3785*****	-0.1418 [NS]	0.110331 [NS]
Wing Beat			0.1209 [NS]	-0.13198 [NS]
Tortuosity				0.059909 [NS]

816
817

818
819
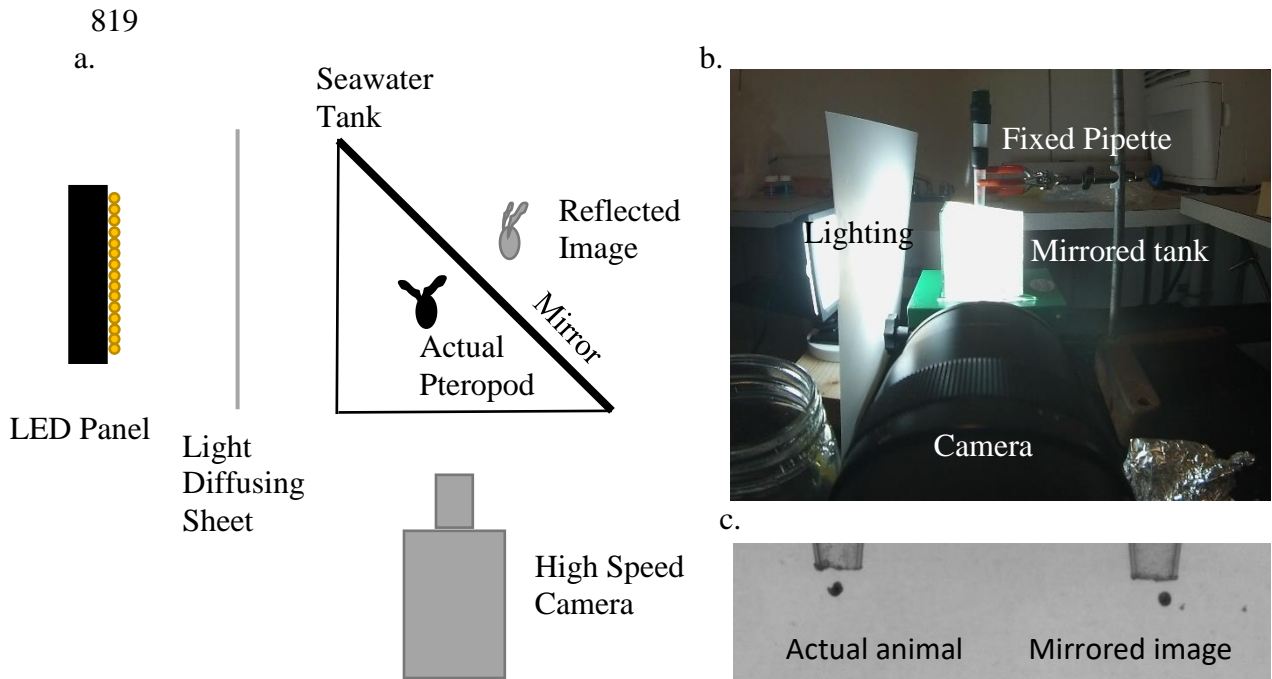
a.

b.

c.

820
821
822   Figure 1. (a) Schematic of the filming set up. The seawater tank had a mirror to show the actual and reflected
823   image of an animal sinking or swimming, allowing position to be determined in three dimensions. A high
824   speed camera was used for filming and illumination was provided by an LED panel. The tank was 10 cm
825   long, 10 cm wide, and 10 cm high. (b) Filming set up showing the mirrored tank with the fixed pipette that
826   was used to drop the pteropods through for sinking trials. (c) One frame of a video shows the actual image
827   and mirrored image of a sinking pteropod with wings withdrawn, shortly after exiting the fixed pipette.
828

829
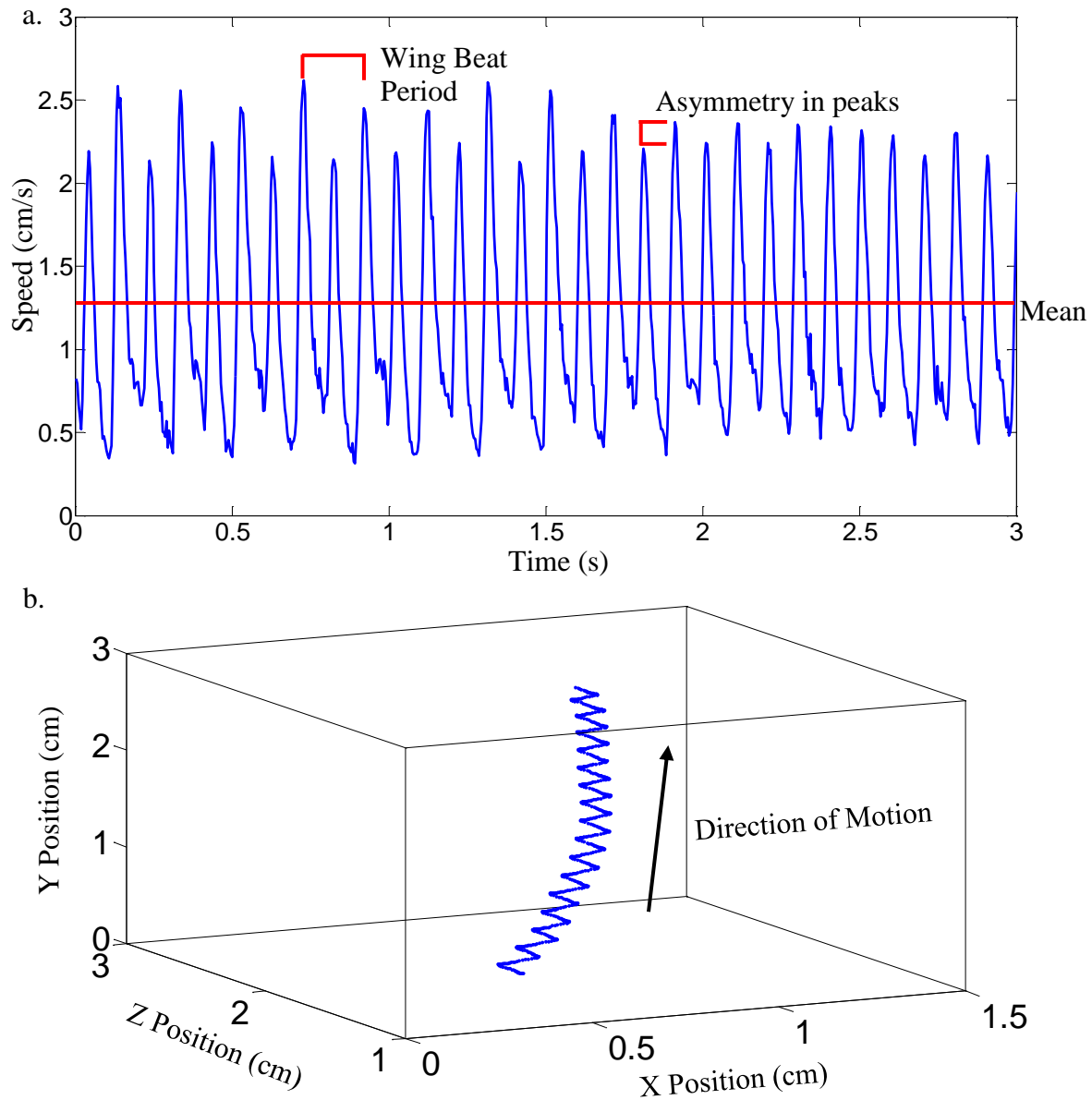
830
831
832 Figure 2. (a) Speed vs time plot of a swimming trial, showing the full time-series of speed from the 3 second
833 video segment (blue), along with calculated mean speed (red line), a wing beat period, and the asymmetry in
834 peaks. The wing beat frequency was calculated as 1/(beat period) and included both the power and recovery
835 strokes. Power strokes were consistently associated with greater speeds and asymmetry between the peak
836 speeds of the power and recovery stroke was measured as the difference between subsequent peaks of speed
837 divided by the larger of the two. (b) The 3D trajectory of a swimming *L. retroversa* shows the pattern of
838 motion. Note that this is a scatter plot but the high frame rate of the camera leads to the points appearing
839 essentially as a line. Tortuosity was calculated as the total cumulative distance traveled divided by the direct
840 distance from starting point to finish.
841
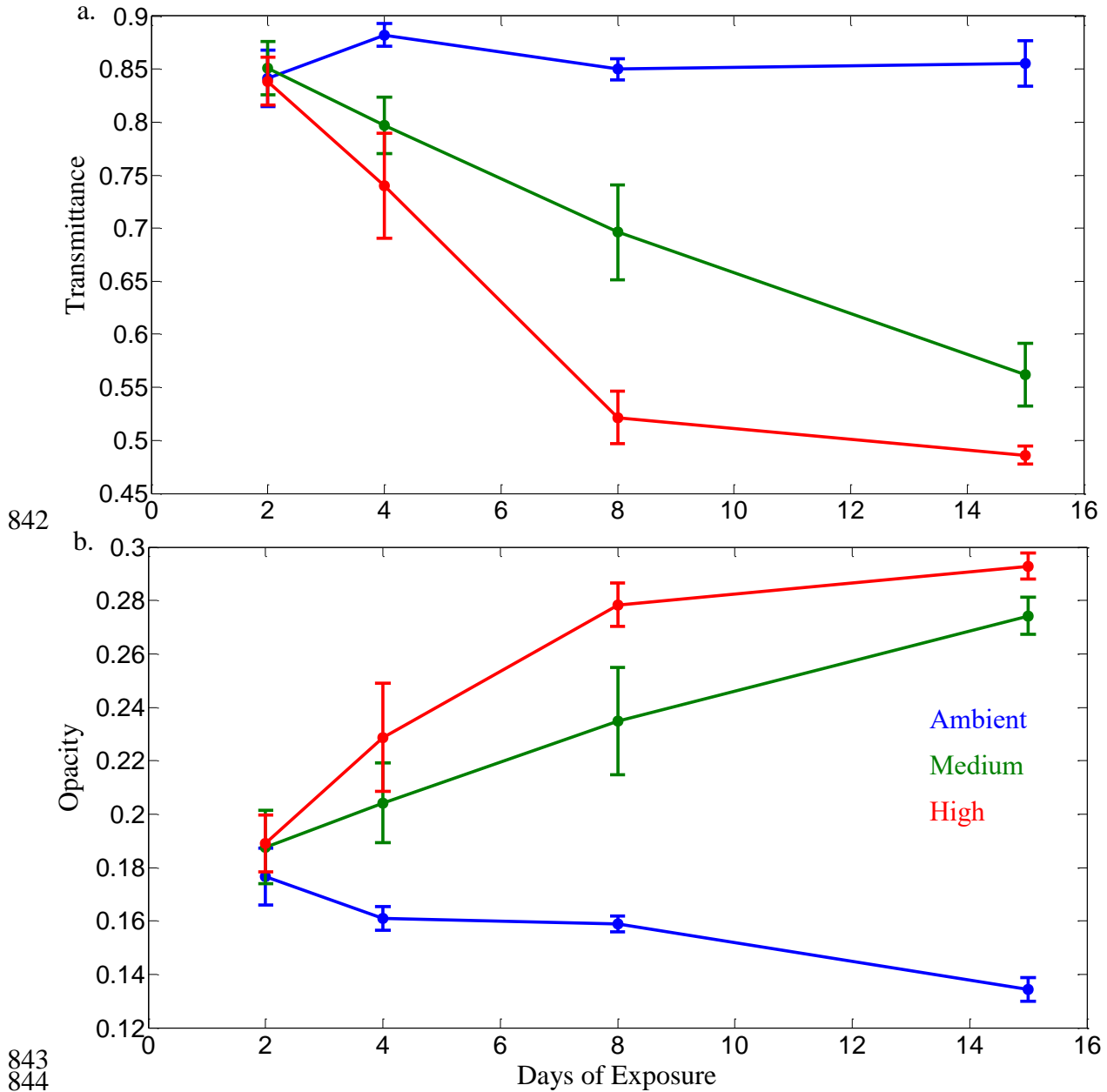
a.

842

b.

843
844
845
846   Figure 3. (a) Transmittance (proportion of transmitted light) and (b) opacity (proportion of reflected light) of
847   *L. retroversa* shells from the April 2015 experiment relative to duration of exposure for each of the three CO_2
848   treatments.
849
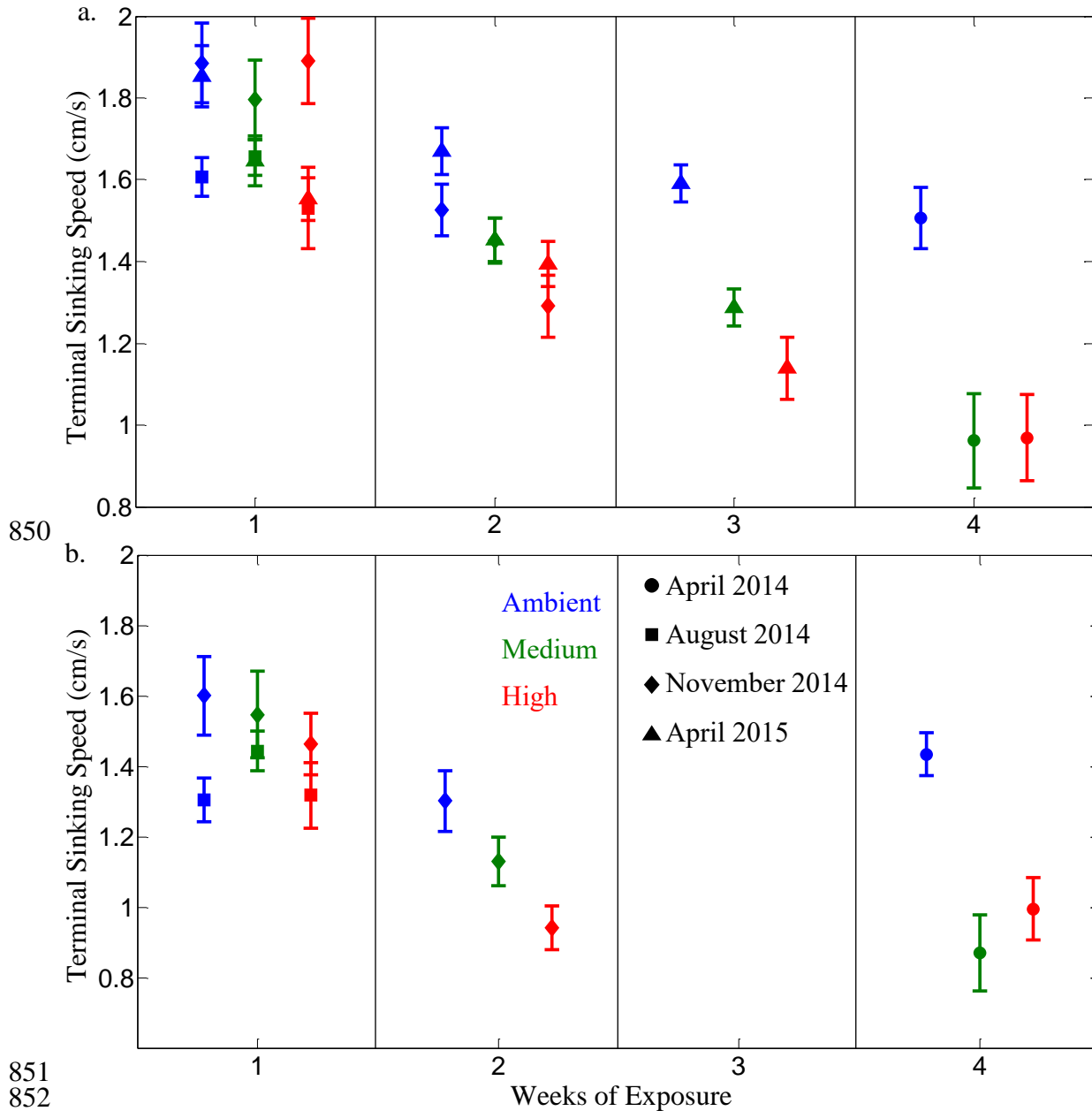
Figure 4. (a) Terminal sinking speed for *L. retroversa* with wings withdrawn for the four experiments (circle: April 2014; square: August 2014; diamond: November 2014; triangle: April 2015) after durations of exposure of 1-4 weeks. From left to right within each weekly bracket the ambient, medium, and high treatment are plotted, although the treatments were measured together of the course of 2-5 days, and are spaced along the x-axis simply for easier visualisation. The error bars denote standard error. (b) The terminal sinking speed with wings extended for the April 2014, August 2014, and November 2015 experiments. No measurements of sinking with wings extended were made in April 2015 or in week 3 of any of the experiments.
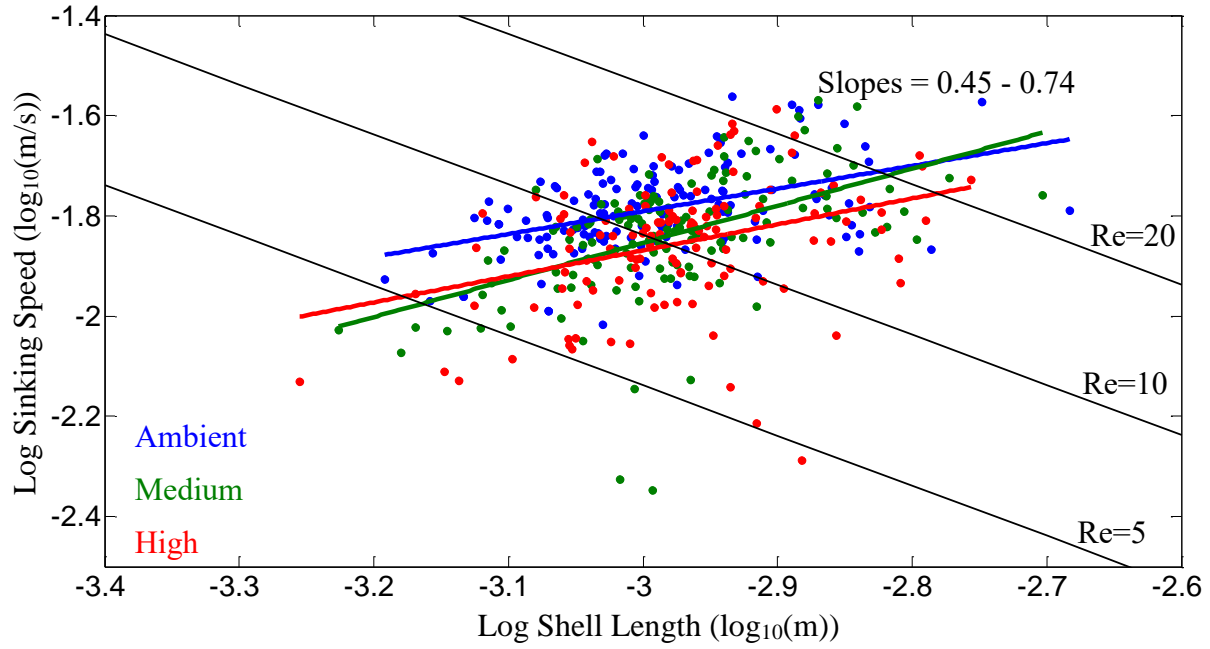
Figure 5. Log$_{10}$ terminal sinking speed with wings withdrawn vs log$_{10}$ shell length for each treatment (points) along with a linear regression for each treatment (lines). The slope of the linear regressions shows the power scaling between sinking speed and shell length. Contours of constant Reynolds numbers (Re) of 5, 10, and 20 are shown in black.
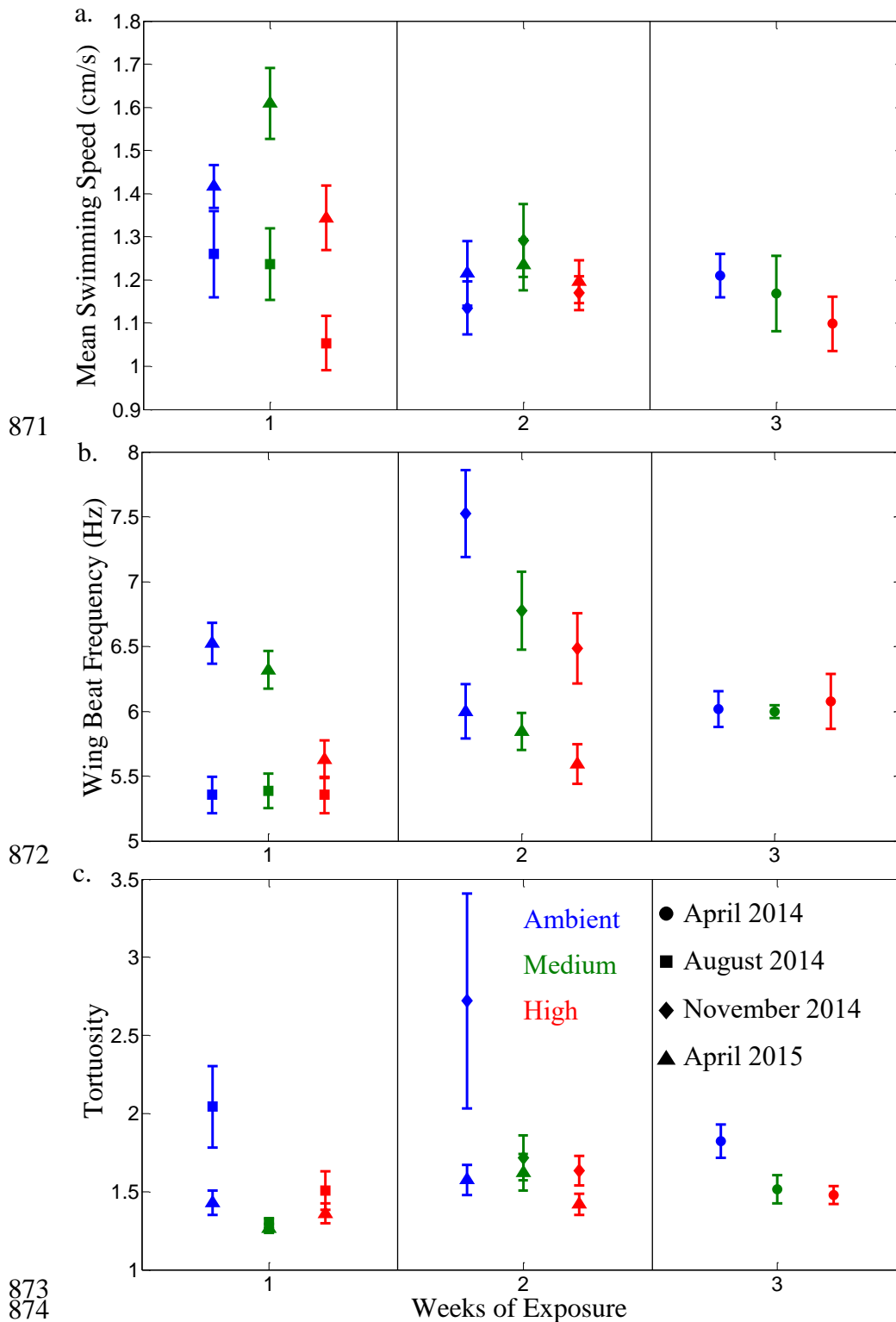
Figure 6. (a) Mean swimming speed, (b) wing beat frequency, and (c) tortuosity for *L. retroversa* for the four experiments (circle: April 2014; square: August 2014; diamond: November 2014; triangle: April 2015) after durations of exposure of 1-3 weeks. From left to right within a week the ambient, medium, and high treatment are plotted, although treatments were measured together over the course of 2-5 days. The error bars denote standard error. Both the power and recovery stroke are included in each wing beat in calculating wing beat frequency.

44

Supplementary Materials

882
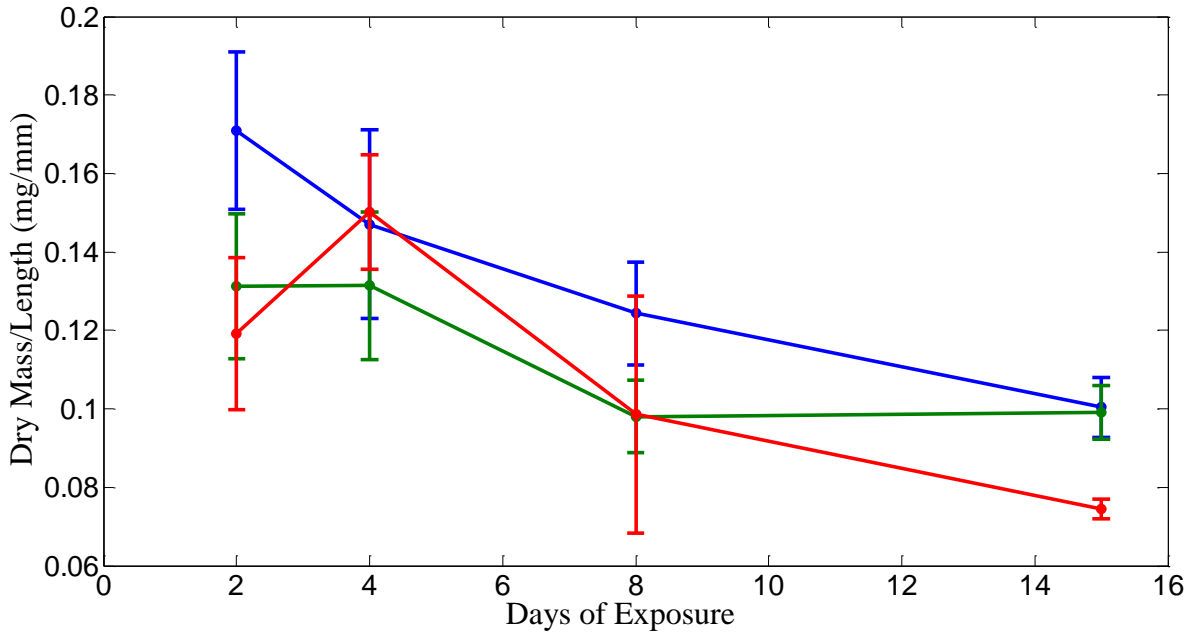
883
884
885 Supplementary Figure S1. Shell dry mass with animal tissue present (i.e., prior to digestion with bleach)
886 normalized to individual length from the April 2015 experiment relative to duration of exposure for each of
887 the three CO_2 treatments.

888
889
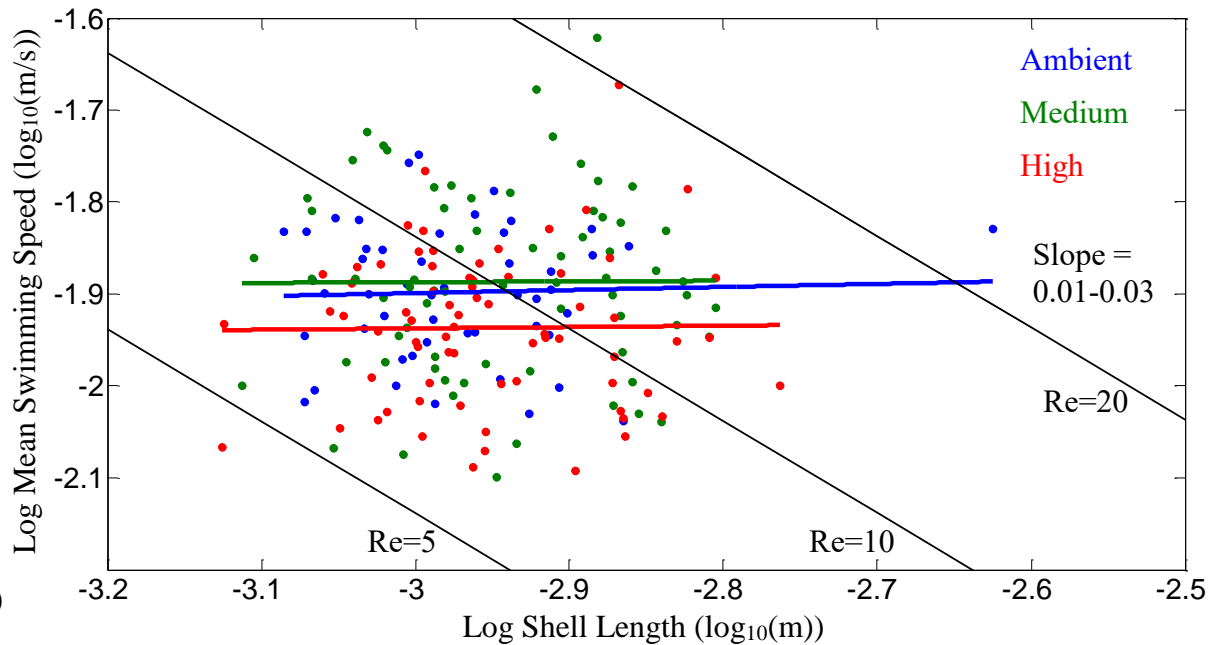
890
891
892
893 Supplementary Figure S2. The $\log_{10}$ mean swimming speed vs $\log_{10}$ shell length (points, coloured according
894 to treatment) along with a linear regression for each treatment (coloured lines). The slopes of the linear
895 regressions indicate the power scaling between swimming speed and shell length. Reynolds numbers (Re) 5,
896 10, and 20 are shown in black lines.
897

898 Supplemental Table S1. Carbonate chemistry parameters measured and calculated over the course of the four
899 experiments for the three treatments: ambient, medium, and high, nominally targeting pCO_2 levels of 400,
900 800, and 1200 µatm, respectively. Water changes happened at weekly intervals, at which time dissolved
901 inorganic carbon (DIC) and total alkalinity (TA) were measured. The TA/DIC measurements of ingoing pre-
902 bubbled water entering the carboys are labelled "In" and the TA/DIC measurements of outgoing water
903 leaving the carboys are labelled "Out". Mid-week measurements of pH were made between water changes,
904 labelled "Mid." "Out" and "Mid" measurements shown are an average of the 2-3 carboys for each treatment,
905 while "In" is a single measurement from the pre-bubbled holding tanks for each treatment. For the ingoing
906 and outgoing water, DIC/TA measurements were used to calculate the values in the last three columns: pH,
907 dissolved CO_2 (pCO_2), and aragonite saturation state (Ω_A). Mid-week measurements of pH were used with
908 the nearest measurement of TA in time to calculate the pCO_2 and Ω_A values to estimate the carbonate
909 chemistry between water changes.

| Cruise | Treat | Day | Water Change | MEASURED | | | CALCULATED | | |
				DIC (µmol/kg)	TA (µmol/kg)	pH	pH	pCO_2 (µatm)	Ω_A
Apr '14	Ambient	0	In	2058	2216	---	8.03	390	1.76
		1	Mid	---	---	7.96	---	470	1.54
		3	Mid	---	---	7.97	---	450	1.57
		5	Mid	---	---	7.99	---	440	1.62
		7	Out	2093	2234	---	7.96	470	1.54
		7	In	2068	2216	---	8.01	420	1.68
		8	Mid	---	---	7.97	---	450	1.58
		10	Mid	---	---	7.96	---	460	1.54
		13	Mid	---	---	7.98	---	440	1.59
		14	Out	2082	2215	---	7.97	460	1.55
		26	Mid	---	---	8.03	---	390	1.77
		29	Mid	---	---	8.03	---	390	1.74
	Medium	0	In	2092	2214	---	7.94	500	1.45
		1	Mid	---	---	7.75	---	790	0.99
		3	Mid	---	---	7.77	---	760	1.02
		5	Mid	---	---	7.78	---	750	1.05
		7	Out	2175	2227	---	7.72	860	0.93
		7	In	2147	2217	---	7.78	740	1.05
		8	Mid	---	---	7.72	---	860	0.92
		10	Mid	---	---	7.70	---	910	0.88
		13	Mid	---	---	7.73	---	830	0.95
		14	Out	2166	2222	---	7.73	830	0.95
		26	Mid	---	---	7.79	---	710	1.09
		29	Mid	---	---	7.80	---	710	1.09
	High	0	In	2111	2215	---	7.88	570	1.31
		1	Mid	---	---	7.59	---	1180	0.69
		3	Mid	---	---	7.61	---	1110	0.73
		5	Mid	---	---	7.68	---	940	0.86
		7	Out	2210	2220	---	7.57	1230	0.67
		7	In	2184	2216	---	7.65	1010	0.80
		8	Mid	---	---	7.57	---	1240	0.67
		10	Mid	---	---	7.55	---	1280	0.65
		13	Mid	---	---	7.58	---	1220	0.68
		14	Out	2202	2219	---	7.60	1150	0.72
		26	Mid	---	---	7.58	---	1200	0.69
		29	Mid	---	---	7.60	---	1150	0.72
	Ambient	0	In	2016	2176	---	8.04	379	1.77

Aug '14		1	Mid	---	---	7.99	---	430	1.58
		3	Mid	---	---	7.92	---	510	1.38
		6	Mid	---	---	7.95	---	470	1.47
		7	Out	2052	2182	---	7.96	460	1.50
		7	In	2028	2183	---	8.03	390	1.73
		8	Mid	---	---	7.99	---	430	1..60
		11	Mid	---	---	7.99	---	430	1.60
		14	Out	2039	2185	---	8.00	414	1.65
	Medium	0	In	2103	2162	---	7.74	790	0.95
		1	Mid	---	---	7.71	---	840	0.90
		3	Mid	---	---	7.69	---	890	0.85
		6	Mid	---	---	7.72	---	840	0.92
		7	Out	2125	2194	---	7.78	750	1.04
		7	In	2104	2180	---	7.80	690	1.07
		8	Mid	---	---	7.70	---	870	0.89
		11	Mid	---	---	7.69	---	900	0.84
		14	Out	2085	2198	---	7.91	540	1.38
	High	0	In	2082	2177	---	7.86	590	1.22
		1	Mid	---	---	7.59	---	1150	0.69
		3	Mid	---	---	7.55	---	1260	0.63
		6	Mid	---	---	7.58	---	1190	0.67
		7	Out	2160	2186	---	7.63	1060	0.75
		7	In	2143	2186	---	7.69	910	0.85
		8	Mid	---	---	7.60	---	1120	0.71
		11	Mid	---	---	7.64	---	1030	0.77
		14	Out	2150	2198	---	7.70	880	0.89
Nov '14	Ambient	0	In	2062	2197	---	7.98	440	1.57
		6	Mid	---	---	8.07	---	360	1.89
		7	Out	2118	2233	---	7.93	520	1.42
		7	In	2066	2195	---	7.97	460	1.52
		8	Mid	---	---	8.01	---	410	1.65
		10	Mid	---	---	7.99	---	430	1.58
		14	Out	2065	2198	---	7.98	440	1.55
	Medium	0	In	2129	2197	---	7.78	730	1.03
		6	Mid	---	---	7.79	---	730	1.06
		7	Out	2234	2234	---	7.55	1320	0.64
		7	In	2142	2194	---	7.73	830	0.92
		8	Mid	---	---	7.73	---	830	0.92
		10	Mid	---	---	7.72	---	840	0.92
		14	Out	2154	2201	---	7.71	870	0.89
	High	0	In	2153	2196	---	7.70	890	0.86
		6	Mid	---	---	7.63	---	1080	0.76
		7	Out	2241	2239	---	7.54	1350	0.62
		7	In	2185	2191	---	7.57	1230	0.65
		8	Mid	---	---	7.58	---	1200	0.67
		10	Mid	---	---	7.57	---	1240	0.64
		14	Out	2205	2206	---	7.55	1290	0.63
Apr '15	Ambient	0	In	2081	2218	---	7.99	440	1.59
		7	Out	2082	2222	---	8.00	430	1.62
		7	In	2077	2212	---	7.98	440	1.58
		7	Mid	---	---	8.01	---	420	1.65
		11	Mid	---	---	7.99	---	430	1.61
		14	Out	2085	2222	---	7.99	440	1.60

		14	In	2108	2257	---	8.01	420	1.72
		16	Mid	---	---	8.02	---	410	1.73
		18	Mid	---	---	8.01	---	420	1.70
	Medium	0	In	2153	2229	---	7.81	700	1.10
		7	Out	2166	2222	---	7.74	820	0.95
		7	In	2147	2211	---	7.77	760	1.01
		7	Mid	---	---	7.79	---	720	1.06
		11	Mid	---	---	7.82	---	680	1.12
		14	Out	2143	2225	---	7.83	660	1.15
		14	In	2173	2253	---	7.82	680	1.14
		16	Mid	---	---	7.79	---	740	1.06
		18	Mid	---	---	7.78	---	750	1.05
	High	0	In	2191	2223	---	7.66	1000	0.80
		7	Out	2208	2221	---	7.59	1170	0.70
		7	In	2208	2209	---	7.55	1300	0.62
		7	Mid	---	---	7.64	---	1050	0.76
		11	Mid	---	---	7.63	---	1070	0.75
		14	Out	2201	2214	---	7.59	1190	0.70
		14	In	2198	2251	---	7.73	850	0.94
		16	Mid	---	---	7.59	---	1190	0.70
		18	Mid	---	---	7.59	---	1200	0.70

910
911